COMAPRING MULTIPLE APPROACHES TO RECONSTRUCTING THE

PHOSPHORUS HISTORY OF MARL LAKES:

A UTAH LAKE CASE STUDY

by

Mark R. Devey

A thesis submitted in partial fulfillment
of the requirements for the degree

of

MASTER OF SCIENCE

in

Watershed Science

Approved:

_____   _____
Janice Brahney, Ph.D.   Dennis Newell, Ph.D.
Major Professor   Committee Member

_____   _____
Diego Fernandez, Ph.D.   D. Richard Cutler, Ph.D.
Committee Member   Interim Vice Provost
     of Graduate Studies

UTAH STATE UNIVERSITY
Logan, UT

2022

ABSTRACT

Comparing multiple approaches to reconstructing the phosphorus history of marl lakes:

A Utah Lake Case Study

by

Mark R. Devey, Master of Science

Utah State University, 2022

Major Professor: Dr. Janice Brahney
Department: Watershed Sciences

Cultural eutrophication driven by excess phosphorus loading is among the greatest threats to freshwater lakes globally. Utah Lake in central Utah, USA is an example of a lake increasingly experiencing cyanobacterial blooms, which are likely a product of cultural eutrophication in recent decades. However, there is uncertainty about how phosphorus loading and concentrations in the lake have changed with modern population growth in the watershed because of the limited water quality data record. To better manage and restore water quality and ecosystem function it is important to understand the timing and magnitude of phosphorus concentration changes in lakes. Because standard methods for reconstructing phosphorus in sediment cores is difficult and imprecise, we tested two novel approaches to measuring lake phosphorus history in one of four sediment cores collected from disparate regions of the lake. Both methods isolate calcium carbonate precipitates to measure co-precipitated phosphorus at intervals throughout the sediment cores. In addition, we performed a more established sequential phosphorus fractionation scheme on all cores. Sequential phosphorus fractionation analysis of four sediment cores taken from Utah Lake supports our hypothesis that P

concentrations have increased across the water column in recent centuries. We find the

Goshen Bay CaCO$_3$-P profile to be the most useful, in part because it reflects a region of

the lake from which harmful algal blooms historically. In this series, the CaCO$_3$-P

fraction of sediments increases by about 100%, corresponding with the timing of modern

human activity in the watershed. The degree of P increases up-core vary spatially across

coring sites. Possible reasons for the differences between coring locations might include

proximity to population centers, susceptibility to disturbance by common carp, and lake

level or climate effects. Because of the loss of historical macrophyte communities

corresponding with population growth and anthropogenic disturbances, Provo Bay and

Goshen Bay were most susceptible to localized disturbance in P cycling. These results

demonstrate the effectiveness of analyzing phosphorus in authigenic calcite as a record of

historical lake phosphorus concentrations.

(61 pages)

PUBLIC ABSTRACT

Comparing multiple approaches to reconstructing the phosphorus history of marl lakes:

A Utah Lake Case Study

Mark R. Devey

Freshwater lakes around the world have suffered from the increasing occurrence of harmful algal blooms in recent decades. One of the most pressing reasons water quality managers try to address harmful algal blooms is that some of the species that occur with them produce toxins which can affect humans, pets, and wildlife. In many lakes, the nutrient phosphorus controls whether these harmful algal and bacterial species can occur. Therefore, efforts to control harmful algal blooms often center around reducing inputs of phosphorus from a variety of sources within the watershed. Scientists and water quality managers have long been challenged by the problem of determining the extent of phosphorus pollution in lakes, and to what degree human activity has changed the phosphorus aspect of aquatic ecosystems. We studied the historical phosphorus record of Utah Lake in north-central Utah, USA, which has been plagued by harmful algal blooms in recent years, by taking sediment cores from four different locations around the lake. We first analyzed the $CaCO_3$ component of one Utah Lake core for trends in phosphorus concentration over time. This approach is based on the co-precipitation of $CaCO_3$ with phosphorus, which scales with concentrations of phosphorus in the lake water. Next, we separated the total phosphorus of samples from four different sediment cores into five different forms by extraction and analyzed each extraction to establish trends in the different fractions of phosphorus that occur in lake sediments In order to

correlate phosphorus trends with important events in the lake's ecological history, we performed cesium and lead isotope analyses, assigning years to the various depths of these sediment cores. These analyses together support our hypothesis that phosphorus concentrations have increased in the lake due to human activity. Nearly all of the phosphorus fractions from each of the four cores increase in more recent years, agreeing with the analyses focused on $CaCO_3$ grains from one specific core which showed an increase in phosphorus beginning around the middle of the 19th century. We recommend applying the principles of our $CaCO_3$-phosphorus analysis performed here in other lakes with $CaCO_3$-P-rich sediments to better understand their ecological histories.

DEDICATION

This manuscript is dedicated to my mother Jennifer, to my late father Scott,

and to my wife Marissa.

ACKNOWLEDGMENTS

Finally, this work wouldn't have been possible without my wife Marissa and the rest of my amazing family who have been nothing but supportive through the long days and short weekends that graduate school has sometimes required.

Mark R. Devey

CONTENTS

Page

LIST OF TABLES

LIST OF FIGURES

INTRODUCTION

Phosphorus (P) is the most common limiting nutrient in freshwater ecosystems (Vollenweider, 1970; Schindler et al., 2016). Many lakes worldwide have become dominated by algae and cyanobacteria due to excess P inputs from human activity, a process known as cultural eutrophication (Schindler, 2012). Given that the trophic state of a lake prior to anthropogenic disturbance is usually unknown, it is useful to be able to determine the magnitude and timing of cultural eutrophication through time. Ordinarily, sediment cores offer researchers insight into various aspects of the history of a water body, but P concentrations have long been a problematic component of sediment cores to reconstruct (Carignan & Flett, 1981). The primary reason for such difficulty is the post-depositional mobility of P brought about by the decomposition of organic matter and the reduction of iron-bound P, which complicates the interpretation of bulk P analyses (Einsele, 1936, 1938; Mortimer, 1941; Carignan & Flett, 1981). The best existing approaches separate sediment P into operationally defined fractions, which means that species are separated based on the reagent used for each extraction (Ure 1991; Bacon and Davidson 2008).. The imprecision of operationally defined fractionation can present challenges for interpreting lake P history. We hypothesize that in lakes where authigenic calcium carbonate precipitation occurs, a more targeted analysis of the $CaCO_3$-P fraction may improve upon or supplement traditional sequential for reconstructing P concentrations in lakes.

Much of the difficulty surrounding reconstructions of P history in lakes stems from its mobility in sediments, meaning that through a variety of mechanisms (e.g. redox reactions, decomposition of organic compounds), P can move vertically in the sediment

profile, typically upwards (Carignan and Flett, 1981; Ostrofsky, 2012; Ginn et al. 2012).

Although these authors and others have identified the issue of P mobility in sediment

profiles, there is little literature attempting to overcome this obstacle from a

biogeochemical approach . The prevailing alternative has been to use diatom-inferred

reconstructions of lake trophic histories, but diatom proxies come with their own sets of

ecological and statistical limitations (Juggins et al., 2013).

One approach to reconstructing lake P history is to develop regional calibrations,

which relate diatom community compositions in sediment cores to P concentrations in the

epilimnion. Such models require a large set of reference sites (as in Bradshaw &

Anderson, 2001, who used 152 sites), as well as validation with lakes having existing P

monitoring data. These requirements preclude lakes with ecosystems distinct from

surrounding lakes, or regions where a low density of lakes limits the potential sample size

of reference sites. Utah Lake, our study site, is an example of a lake for which diatom-

inferred P calibrations are not appropriate because it is geologically and ecologically

dissimilar to nearby lakes, being neither alpine nor terminal.

Other researchers have turned to sequential extraction methods, first developed

for studying soils, to overcome the issue of analyzing only TP in bulk sediments. Ure

(1991) defined three types of chemical speciation. The first type, classical speciation,

defines based on specific chemical compounds or oxidation states. The second type,

functional speciation, categorizes based on function (e.g. plant bioavailable). The third,

operational speciation, distinguishes fractions only by the reagents used in the extraction.

Bacon and Davidson (2008) emphasize that the latter is a common limitation for

sequential fractionation. Most sequential fractionation serves only to define operational

groups which must be interpreted. For instance, a hydrochloric acid-extractable fraction may target a trace element in carbonate minerals, but unintentionally release the element from non-target fractions as well, such as organic matter. Still, the fact that operationally defined fractions do not correspond perfectly with target compounds need not be prohibitive; rather, it is a caveat to an approach that is useful for drawing certain conclusions (Bacon and Davidson, 2008).

The significance of $CaCO_3$-P analysis as an alternative to existing methods for reconstructing the P history of marl lakes lies in its authigenic nature. Although hydrology, source material, and climate must be suitable for marl lakes to form, the process of authigenic $CaCO_3$ precipitation is generally biologically mediated. Just as in marine carbonates, authigenic carbonate in marl lakes can form when invertebrate species precipitate $CaCO_3$ to form shells (Dean 1981). In addition, the fine-grained $CaCO_3$ which comprises marl sediments is a product of photosynthesizing microbiota such as the picoplankton *Synechococcus*. While it is possible for abiotic drivers (e.g. temperature, evaporation) to initiate $CaCO_3$precipitation, Thompson et al. (1997) found that the microenvironments characterized by high pH and Ca^{2+} concentrations surrounding *Synechococcus* cells explained large-scale calcium carbonate precipitation across a temperate marl lake. Photosynthetic activity in the benthic zone (Thiel et al., 1997) as well as among macrophytes (Pełechaty et al., 2013) has a similar effect.

As it precipitates, $CaCO_3$ contributes to the mineralization and, in many cases, permanent burial of P. Although P is not part of the formal structure of calcium carbonate, the co-precipitation of P with $CaCO_3$ has been documented in the laboratory setting as well as in lake systems. Ishikawa and Ichikuni (1981) describe the mechanism

whereby phosphate co-precipitates with $CaCO_3$ as the replacement of 3 CO_3^{2-} ions by 2 PO_4^{3-} ions in the ion exchange equilibrium:

$$3(CO_3^{2-})_S + 2(PO_4^{3-})_L \rightleftharpoons 3(CO_3^{2-})_L + 2(PO_4^{3-})_S$$
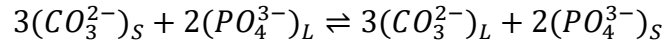
Where S represents $CaCO_3$ and L represents aqueous solution. Ishikawa and Ichikuni (1981) found further evidence that within the crystal, phosphate is distributed homogeneously. Their experiment demonstrated the uniform distribution of phosphate within the calcite crystal structure by fractionally leaching calcite crystals containing phosphate. Throughout the leaching experiment, the percent dissolved Ca^{2+} equaled the percent dissolved PO_4^{3-} , indicating that the distribution of both ions was constant throughout the crystal. Co-precipitation is notably different from simple adsorption onto $CaCO_3$ grains, as the former can only be released by dissolution.

In controlled laboratory precipitation, there is a linear relationship between P concentrations in aqueous solution and P in calcium carbonate which precipitates from that solution (Devey & Brahney, 2019). This relationship is the basis for our $CaCO_3$-P - focused analysis, but does not extend perfectly to natural lake systems, where the presence of Mg^{2+}, and other ions to lesser degrees, affect the rate and resulting polymorph of $CaCO_3$ precipitation and P scavenging (Kitano et al. 1978). Calcium carbonate co-precipitation with P occurs when lakes experience whiting events, or large-scale calcium carbonate precipitation (Otsuki and Wetzel, 1972; Murphy et al., 1983; Kleiner, 1988). Calcium carbonate serves such a major role in the P budgets of hardwater lakes that an increasing P concentration can serve as a negative feedback mechanism. Rising nutrient levels lead to greater primary productivity, including

populations of picoplankton (e.g. *Synechococcus*), which create the microenvironments suitable for $CaCO_3$ to precipitate and scavenge phosphate from the water (Hamilton et al., 2009). Here we test and compare two methods for extracting $CaCO_3$-bound P using a test system, Utah Lake, which has experienced harmful algal blooms with increasing frequency in recent years. The first is part of a broader sequential P fractionation analysis, and the second is a two-pronged approach to effectively isolate $CaCO_3$-P for analysis. We hypothesize that each of these methods will show an increase in water column-P corresponding with modern development and concomitant population growth in the watershed.

MATERIALS AND METHODS

Study Site

Utah Lake, located in north-central Utah, USA, represents one of only a few shallow remnants of Pleistocene Lake Bonneville (Gilbert, 1890; Oviatt 1997). Many characteristics of the lake are controlled by its shallow average depth (2.8 m), which allows for frequent, widespread re-suspension of sediments by wave action. The geology of the lake is also characterized by $CaCO_3$-rich sediments. X-ray diffraction (XRD) analysis by Randall et al. (2019) found that the $CaCO_3$ composition of sediments ranged from 12.7- 75.1% (45.9% ± 4.1%; mean ± standard error), and using sequential extraction techniques determined it accounts for 25-50% of P storage in sediments (Randall, 2017).

The increasing prevalence of summertime harmful algal blooms in Utah Lake (Utah Department of Environmental Quality, 2007), has brought attention to the causes and extent of its cultural eutrophication. A simple timeline of relevant events in the history of the Utah Lake watershed is given in figure 1. Because the introduction of modern settlements and ensuing population growth begins in 1849, it is likely that increases in the sediment P profile might begin around this time because as towns began to develop around the valley, drainage ditches were built to move raw sewage to the lake. Although wastewater treatment plants (WWTPs) were eventually constructed around the 1950s to address nutrient pollution at the time, P inputs from wastewater would still have increased after their construction corresponding with sheer population growth. Although there was awareness of the need to curb nutrient pollution in the middle of the 20th century, the Utah Lake water quality data record is virtually nonexistent prior to 1960, and does not come about in a robust way until the 1970s (Judd, 1997). As a result, there

is a substantial period of surface water P history, including pre-disturbance conditions, for which there is no data. The P loading calculated to determine total maximum daily loads (TMDLs) of P for Utah Lake were gathered from 1980-2003, which determined that 227.8 tons year^{-1} are loaded into the lake by WWTPs, or 76.5% of the total. Although this is a substantial portion of the P budget, it is difficult to know to what extent this increase has ultimately changed the lake's trophic state without any pre-disturbance data for reference.
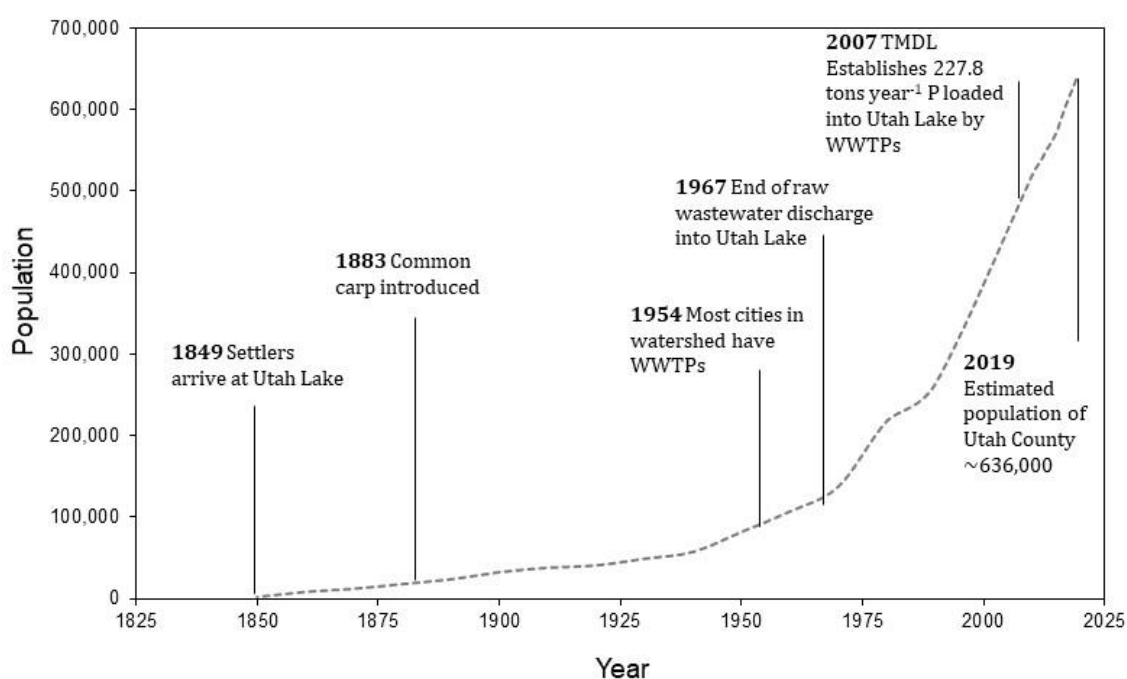
Figure 1. Timeline of important events in Utah Lake regarding phosphorus inputs and trophic status. The dashed line shows estimated population growth since the arrival of western settlers.

Randall et al. (2019) studied the spatial distribution of TP in Utah Lake surface sediments (approximately the top 5 cm) and found that TP varied from 280 to 1710 mg/kg, with the highest concentrations clustered around the eastern shore near population

centers. The authors further noted the high concentrations of pore water P compared to water column P, suggesting that legacy P from sediments may contribute to P cycling in the lake. This effect also illustrates the high mobility of P in bulk Utah Lake sediments which makes paleolimnological study difficult.

Because calcium carbonate is a primary component of Utah Lake sediments, they are ideal for testing a novel approach to measuring P in lake sediments by isolating $CaCO_3$-P. Randall et al. (2019) found the HCl-extractable fraction (operationally $CaCO_3$-P) to account for much of the P storage in Utah Lake's surface sediments. The combined sequential extraction data from the above authors with palaeoecological data from King (2019) offer potential references with which to cross-validate my results. Additionally, there is an impetus from stakeholders to better understand the biogeochemical history of the lake as it pertains to future nutrient management decisions.

We collected four sediment cores for this study, each taken from a site with some physiographical or ecological significance to Utah Lake (figure 2). Of these four, one was collected in 2018 near Bird Island to represent the deepest part of the lake as well as the pelagic zone. The second was collected 2018 in Goshen Bay, a region which once supported communities of macrophytes, but where concentrated harmful algal blooms (HABs) have occurred in recent years. The third was a shorter core collected from the northern part of the lake in 2019, far from the sites of recurring HABs as well as water treatment plants. Finally, a core was collected in 2020 from Provo Bay, which is the source from which many HABs in the lake proceed.

Core Collection and Description

Each sediment core was collected using a Livingstone/Bolivia piston coring system. Cores were shipped to the Continental Scientific Drilling (CSD) facility at the University of Minnesota for splitting, archiving, sub-sampling (Bird Island and Goshen only), and an initial core description. The age of sediments with respect to depth will be established from ^{137}Cs using Bayesian age-depth modeling for Goshen Bay and Provo Bay, and ^{210}Pb dating for Bird Island (Blaauw and Christen, 2011). Upon returning to our facility at Utah State University, the North and Provo Bay cores were subsampled for analysis. All were kept refrigerated at 4 °C prior to use.
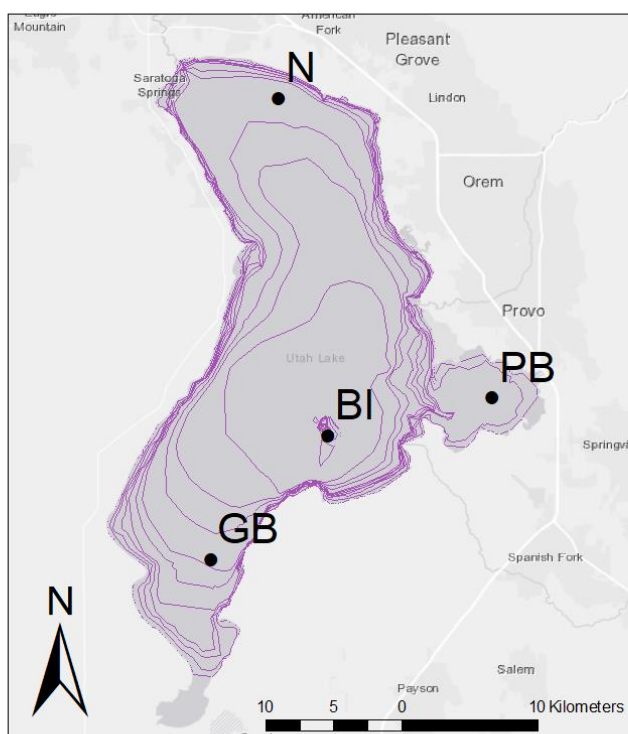
Figure 2. Locations of four cores collected from Utah Lake. Locations include Goshen Bay (GB; 40.1086°, -111.8751°), Bird Island (BI; 40.1712°, -111.7998°), North (N; 40.34070, -111.83026), and Provo Bay (PB; 40.17118°, -111.79978°).

We characterized and described the core according to a series of standard physical and chemical measurements prior to phosphorus analysis. Cores were sent to the National Lacustrine Core Facility (LacCore) at the University of Minnesota for splitting, archiving, and initial physical description. Subsamples of the Bird Island core and Goshen Bay cores were sent to Queen's University Facility for Isotope Research, Kingston, ON, Canada for ^{137}Cs isotope dating. Because of COVID-19-related laboratory closures, our later analysis of the Bird Island and Provo Bay cores for ^{210}Pb and ^{137}Cs, respectively, were performed at LANSET, University of Ottawa, Ottawa, ON, Canada.

Sediment texture and Munsell color were described prior to sectioning each core. A 1 cm^3 subsample was taken at every 1 cm of depth, and analyzed for wet and dry density, as well as loss-on-ignition at 550 and 1000 °C. Each core was sectioned in 0.5 or 1 cm intervals and thereafter stored in Whirlpak® bags. The presence of macrofossils, including floral and faunal remains, were cataloged during core sectioning.

Sequential Fractionation

Our sequential fractionation scheme consisted of five increasingly harsh reagents and process, dividing TP into five operational fractions (table 1). Subsamples were freeze-dried and weighed in plastic centrifuge tubes prior to extractions. Each individual sample had a volume of extractant applied proportional to the mass of the sample so that the mass-to-volume ratio remained constant. The exact volume of extractant applied to each sample was calculated by weighing the liquid and converting it to volume from a known density.

Table 1 summarizes the reagents used, basic process, and expected P forms as well as what type (SRP, NRP, TP) of P was analyzed. The first step extracts P loosely

adsorbed to particle surfaces, exchangeable P, and porewater P, using 1 M magnesium chloride ($MgCl_2$). Salts such as $MgCl_2$ are used in extraction schemes to extract P by either the formation of a $MgPO_4^-$ complex or displacement by the Cl^- ion. In the second step, the citrate bicarbonate-dithionite solution is meant to extract the fraction of P which is bound to reducible forms of Fe and Mn. A mixed solution of trisodium citrate, sodium bicarbonate, and sodium dithionite ("BD") reduces oxidized species of Fe and Mn, thereby releasing adsorbed P from Fe/Mn oxides and hydroxides. Citrate acts as a chelator, complexing metal ions. When used early in the sequence, CDB has the benefit of not disturbing P associated with clays or organic compounds. However, citrate has a strong affinity for Ca and may extract some P loosely bound to the exterior of calcium minerals (Broberg and Persson 1988).

The third step uses sodium hydroxide (NaOH) to extract P by hydrolysis from a broad fraction generally termed "biogenic", which consists of P in microorganisms, polyphosphates, detritus, humic acids, and other organic compounds (Hupfer et al. 1995). It also extracts P bound to Al oxides (Al-P) and any P exchangeable with OH^-. Biogenic P is distinguished from Al-P in this approach by:

$$TP = SRP + NRP$$

Non-reactive phosphorus (NRP) is calculated as the difference of total P (TP) and soluble reactive P (SRP). NRP corresponds with biogenic P and SRP corresponds with Al-bound and OH^- exchangeable P.

The fourth extraction is dilute hydrochloric acid, targeting the more readily soluble forms of $CaCO_3$-P, including amorphous Ca minerals, biogenic calcium

carbonate, crystalline calcium carbonate precipitates, and possibly authigenic apatite. A

0.5 M HCl solution will not dissolve any detrital apatite in the sediments. This fraction is

considered not bioavailable.

Finally, the refractory P extraction targets biogenic compounds which are

otherwise resistant to extraction, including some phosphate esters and phosphonates

(Ingall et al. 1990; Broberg and Persson 1988). Although this fraction is, by definition,

not bioavailable and is generally considered a permanent P pool, it is important for

understanding the relative makeup of total sediment P, except for recalcitrant mineral P,

which is not considered in this study. Whereas many studies use wet persulfate digestions

to extract total P, I opted to use dry oxidation by combusting my samples at 550° C,

followed by extraction with 1 M HCl. This decision is based on evidence that wet

persulfate digestions underestimate TP (Zhang 2012).

Table 1. Summary of the sequential fractionation scheme used on all four cores, adapted from a scheme suggested for $CaCO_3$-rich lake environments by Hupfer et al. (2009). Another study on Utah Lake sediments, Randall et al (2019), also used a similar approach.

Step	Reagent	Concentration	Time	Expected P Forms
1	$MgCl_2$	1.0 M	0.5 h	(SRP) P loosely adsorbed to the surfaces of particles; immediately available P
2	Sodium Bicarbonate Sodium Dithionite Trisodium citrate	1.0 M 0.14 M 0.3 M	16 h	(TP) Reducible P forms, especially bound to Fe and Mn
3	NaOH	1.0 M	16 h	Al-bound P (SRP) and P in organic material (NRP), including P in detritus, P bound to humic compounds, and P in microbes
4	HCl	0.5 M	16 h	(TP) Ca-P, especially calcite-P co-precipitates
5	Ignition at 550 °C HCl	1.0 M	16 h	(TP) Refractory P

In addition to our main sequential P fraction analysis, we performed the P extraction scheme on a set of subsamples from SRM 2702 (Inorganics in Marine Sediment) to determine absolute efficiency of our analyses, as well as variability. We also subsampled several intervals from the Bird Island and Goshen Bay cores for total P analysis for comparison with the sum of individual fractions. Applied to the SRM marine sediment material, this procedure was ~56% efficient at extracting total P across all five fractions. The remaining 44% is assumed to be in resistant mineral phases, which we do not expect this procedure to be able to extract because this procedure does not go as far as a complete digestion of the sediment material. The results of our total phosphorus to sum of fractions comparison and SRM analysis are provided in detail in appendices 6-8. After completion, the $MgCl_2$ and NaOH extracts were analyzed for SRP on a SpectraMax$^{®}$ M2 using the molybdenum blue method. The bicarbonate-dithionite, NaOH, and both HCl extracts were analyzed for TP using an Agilent Triple Quadrupole ICP-MS at the ICP-MS Metals laboratory at the University of Utah, Utah, USA, as well as by the same instrument at the Department of Geosciences at Utah State University. The non-reactive P (NRP) in the NaOH extract was obtained by subtracting SRP from TP.

Energy-dispersive X-ray Spectroscopy

To determine $CaCO_3$-bound phosphorus concentrations, samples were digested in 30% hydrogen peroxide for 72 hours to remove organic matter and organic-associated P, rinsed with a $MgCl_2$ solution, then rinsed in ultrapure water to remove any weakly-adsorbed P. The material was then suspended again in ultrapure water and drop cast onto silicon wafers for analysis. The mounted samples were then carbon coated to improve

conductivity for better results. Because silicon and carbon were introduced into the sample as mounting medium and coating, respectively, they were removed from the final elemental spectra.

Scanning electron microscopy (SEM) was conducted with a FEI Quanta FEG-650 SEM operating at 10 kV accelerating voltage. Energy Dispersive X-ray spectroscopy (EDS) was performed with an Oxford X-Max detector, attached to the FEI Quanta FEG, at 10 kV. Sample solution was drop-casted onto 10 x 10 mm Si-chip substrate to make a thick film, air dried then 10 nm carbon coated via thermal evaporation using EMS-150 ES metal/carbon coater, before placing in the SEM chamber.

Once under the SEM, we arbitrarily chose an area on the sample mount and mapped the image for constituent elements, including oxygen, carbon, silicon, calcium, and any other trace elements the instrument could detect (up to parts per thousand). From these maps (as in figure 4), it was possible to distinguish grains by approximate composition, including calcium carbonates, calcium-magnesium carbonate, phosphates, aluminosilicates, and iron oxides. From these maps, we selected ten grains which, based on relative composition, were most likely calcium carbonate grains for EDS analysis. We allowed each grain 3×10^6 counts to detect P at 10 kV energy and 10,000x magnification. If, after all counts were completed and the software was not able to confirm the presence of P at the given point and we consider the sample to be < 0.0% P by weight, or a nondetect.

We analyzed approximately ten randomly selected $CaCO_3$ grains for each of the intervals sampled (see table X). Because sample G1 (0-2.5 cm) had by far the greatest P concentration, as well as no nondetects (or "left-censored" P concentration values), the

same sediment drop cast was analyzed again on a different day, selecting a different

random set of CaCO₃ grains. We also collected spectra for several non- CaCO₃ grains

during this exploration, particularly where P was concentrated according to the elemental

map. It was relatively easy, using this method, for us to avoid concentrations of iron or

aluminum, where P was often concentrated much more than in CaCO₃. We were also able

to distinguish apatite grains by the presence of fluorine and very high concentrations of P.

Size-separate CaCO₃-Phosphorus Analysis

We used a novel, improved approach to analyzing CaCO₃-P by using a less harsh

extracting reagent on a more targeted size fraction of sediments. Analysis of the grain

size distribution of mineral types using the SEM/EDS indicated that the authigenic

CaCO₃ in the Goshen Bay core belonged to a size class that was distinctly finer than most

detrital grains. Bulk sediments were ignited at 550 °C in acid-washed crucibles to release

organic and refractory P, then vortexed and sonicated in a MgCl₂ solution to break up

clumps and remove loosely-adsorbed P. Following the MgCL₂ rinse, samples were triple-

rinsed in ultrapure water, then filtered to isolate the 0.45-10-micron fraction. Using

ultrapure water and a vacuum system, the sediment material was separated using a 10 µm

Nitex mesh filter. The suspended <10 µm fraction was collected onto a 0.45 µm cellulose

acetate filter and put in a desiccator to dry. The filters were then placed into

polypropylene centrifuge tubes, dried again at 110 °C, and weighed.

With this modified extraction procedure, we sought to address the issue that the

HCl reagent used in typical sequential extraction schemes risks carry-over from other

fractions. A buffer solution (pH=4.5), which could still dissolve CaCO₃ but at a much

higher pH, was used to dissolve calcium carbonate from the isolated 0.45-10 µm fraction

captured on the filters. Seven mL of the buffer solution was added to each sample tube

and shaken for 48 hours at 20 °C. The mixture was centrifuged and extracted, and the

remaining detrital sediment and filter paper were rinsed, dried, and weighed again to

obtain a total mass of dissolved sediments. This dissolved material was assumed to be

primarily carbonate material. The extract was analyzed via quadrupole ICP-MS for

phosphorus and a suite of metals typically associated with carbonate minerals (Ca, Mg,

Ba, Sr, Mn, and Fe).

RESULTS

Core Descriptions

Figure 3 outlines the weight-percent organic matter (loss on ignition [LOI] 550 °C) of each of the four cores along with units demarcated by shifts in loss on ignition and fossil content. The North, Goshen Bay, and Bird Island cores are all composed of relatively similar sedimentary textures, carbonate mud to carbonate silt, although LOI and sediment moisture content profiles reveal a moderate level of variability in these three cores, with North being the most consistent (figure 3; appendices 2-4). The Provo Bay core exhibits stark changes in not only LOI and moisture profiles, but in color as well. in texture and composition from one another.
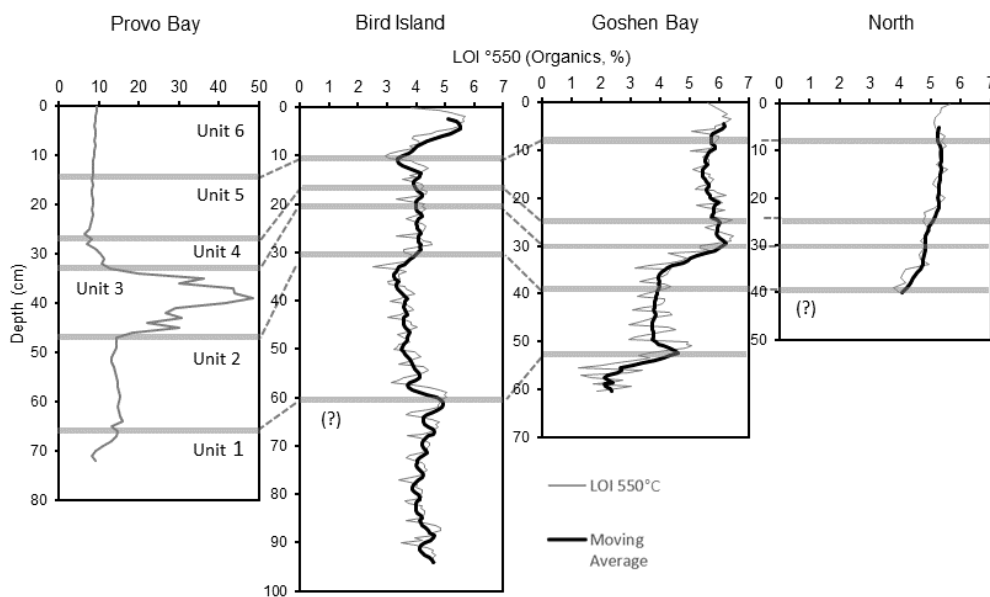
Figure 3. Loss on ignition profiles (550 °C) for each of the four cores, taken at 1 cm intervals (Provo Bay and North) and 0.5 cm intervals (Bird Island and Goshen Bay). This figure is annotated with approximate units based on LOI profiles and other elements of the core description, including sediment color and texture. Unit 1 is difficult to discern in Bird Island because the modeled dates do not extend throughout the entire core, and there were no dates for the North core. LOI data for Goshen Bay and Bird Island were collected by King (2019).
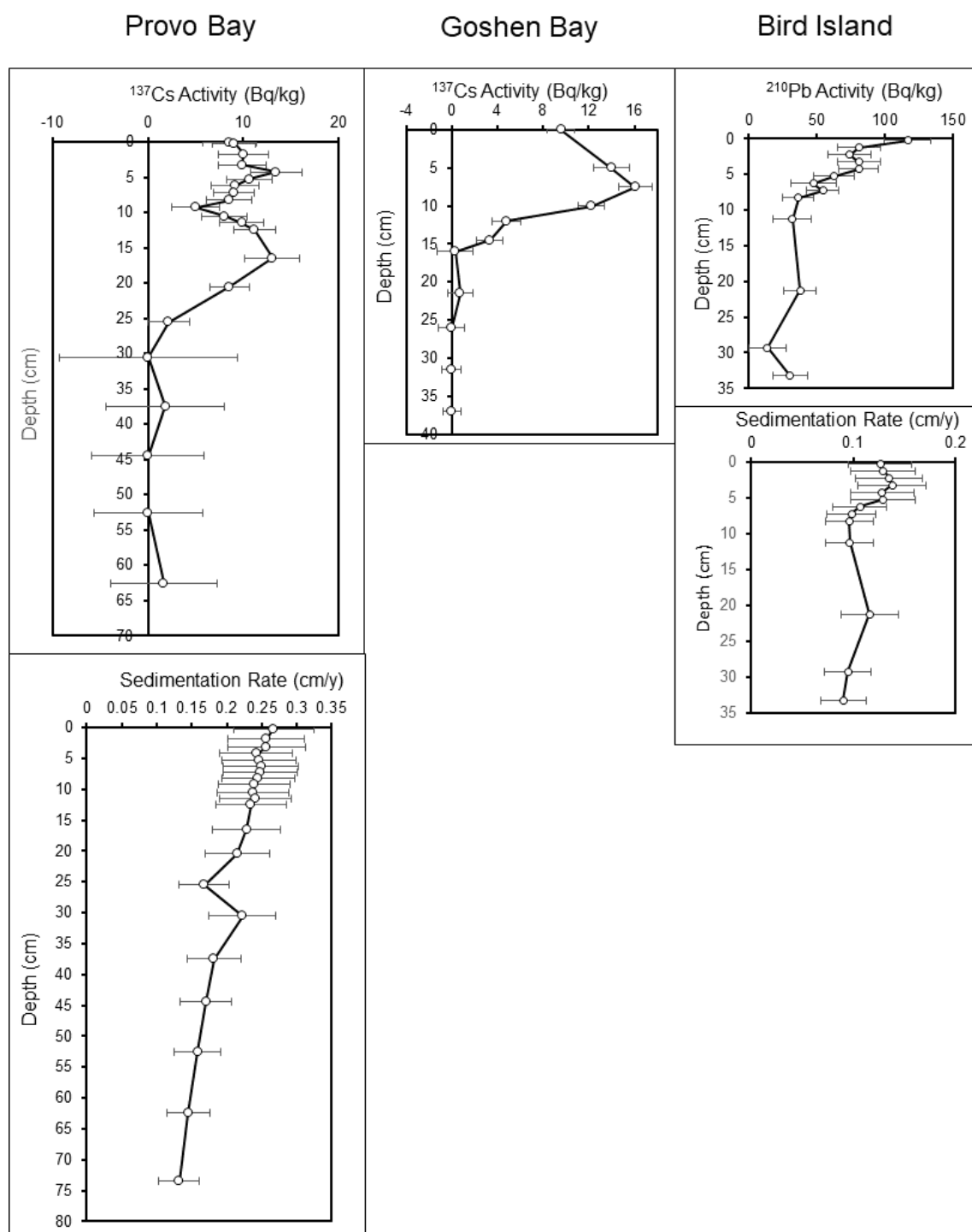
Figure 4. Isotope activity profiles used in the dating models used to generate age-depth relationships in this study, as well as sedimentation rates (Bird Island and Provo Bay). Sedimentation rates were not modelled for Goshen Bay. [137]Cs was used for Provo Bay and Goshen Bay, whereas ^{210}Pb was a more useful model for Bird Island.

Sequential Phosphorus Fractionation

The Goshen Bay core exhibited a steady increase in $MgCl_2$-extractable P between from about 4 to 13 mg/kg. The BD-extractable P varied throughout the profile from as high as 168 mg/kg to below reagent blank values. NRP in the NaOH-extractable fraction started in the 4 mg/kg until about 1857, after which point this fraction approximately doubled, peaking as high as 19 mg/kg. Only a few of the HCl extracts had detectable levels of phosphorus, exhibiting no apparent trend. The refractory P fraction exhibited by far the most concentrated P, ranging between around 500 and 100 mg/kg. There was one peak that corresponded with a peak in NaOH-NRP, and a trough that corresponded with a trough in BD-extractable P.

The Bird Island core showed modest increases in $MgCl_2$-extractable P up-core, on the order of 3-13 mg/kg. In a similar fashion to the Goshen Bay core, BD-extractable P showed much variability and no apparent trend, except for peaks around 9 and 21 cm, which corresponded with peaks or troughs in subsequent fractions. The NaOH-NRP exhibited variability between 5-15 mg/kg, with a trend somewhat inversely correlated with the HCl extract. The 0.5 M HCl-extractable fraction remained at or near detection limits until increasing at 55 cm to the 100-mg/kg P range, and increasing again around 30 cm to the 300-400 mg/kg range until peaking at 9 cm to over 1200 mg/kg P. The refractory P fraction also exhibited strong peaks at 94, 21, and 11 cm, but otherwise stood on the order of 100-1000 mg/kg P.
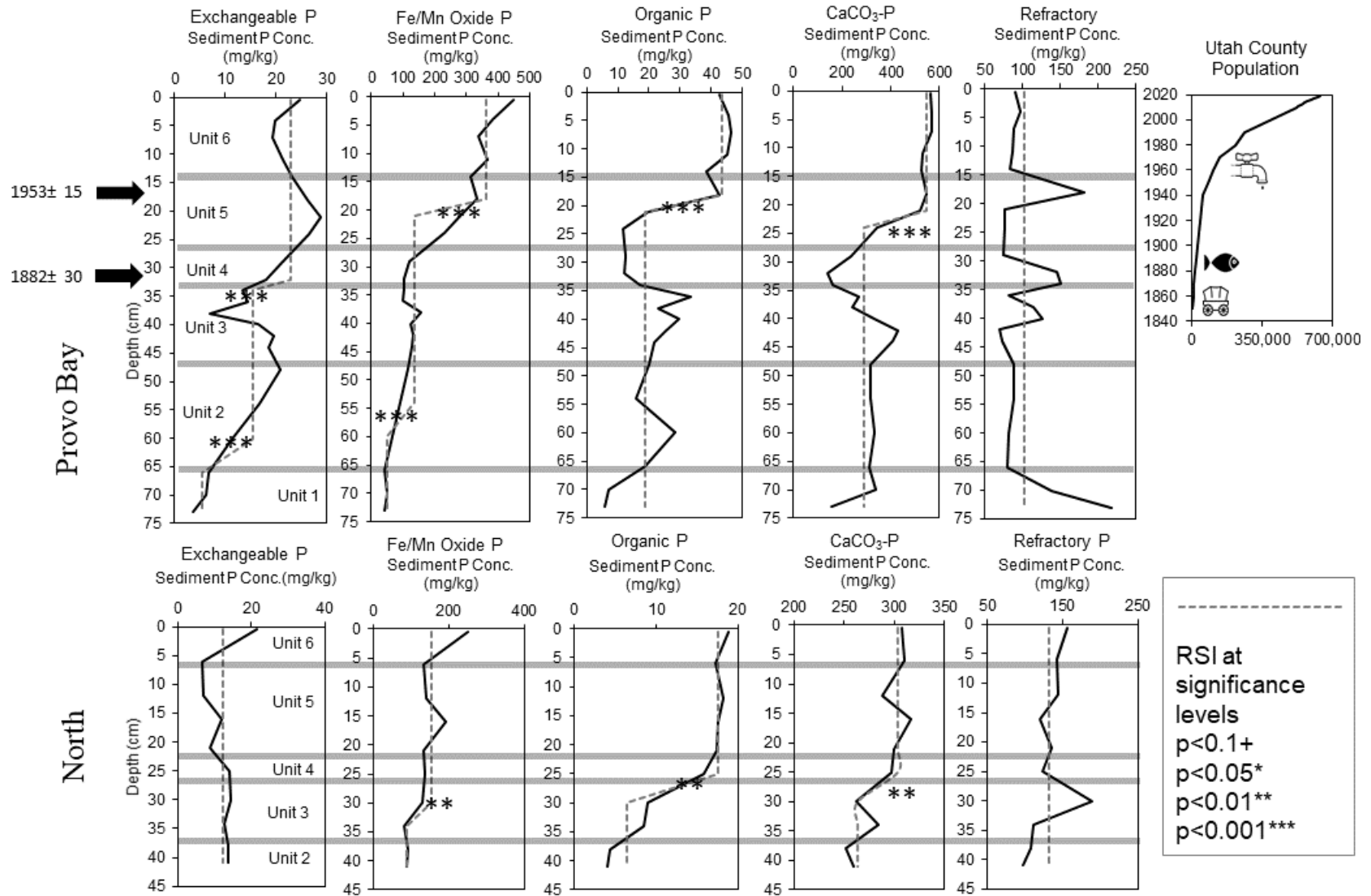
The North core $MgCl_2$-extractable P decreased gradually from 14-7 mg/kg until the topmost interval, where it increased sharply to over 20 mg/kg. Both the BD and NaOH-NRP increased up-core, from 88 to 250 and 4 to 19 mg/kg, respectively. The 0.5

M HCl-extractable fraction increased only slightly, but with little variability, from 259 to 309 mg/kg. Refractory P increased from 97 to 143 mg/kg, with one outlier peak of 189 mg/kg at 30 cm.

Each P fraction in the Provo Bay core saw some degree of increase up-core except for the refractory fraction. $MgCl_2$-extractable P increased from about 4 to 25 mg/kg, dipping midway around 1850. BD-extractable P increased from about 40 to 450 mg/kg. NaOH-NRP increased from 6 to as high as 46 in newer deposits, with more variability than in the first two fractions. HCl-extractable P experienced a very similar-shaped profile to NaOH-NRP but increased from about values in the low 300 mg/kg range to values in the 560 mg/kg range. The refractory P profile centered around 90 mg/kg, except for one peak at the bottom of the profile (second half of the 17th century), two small peaks in the mid to late 19th century, and again in 1946.
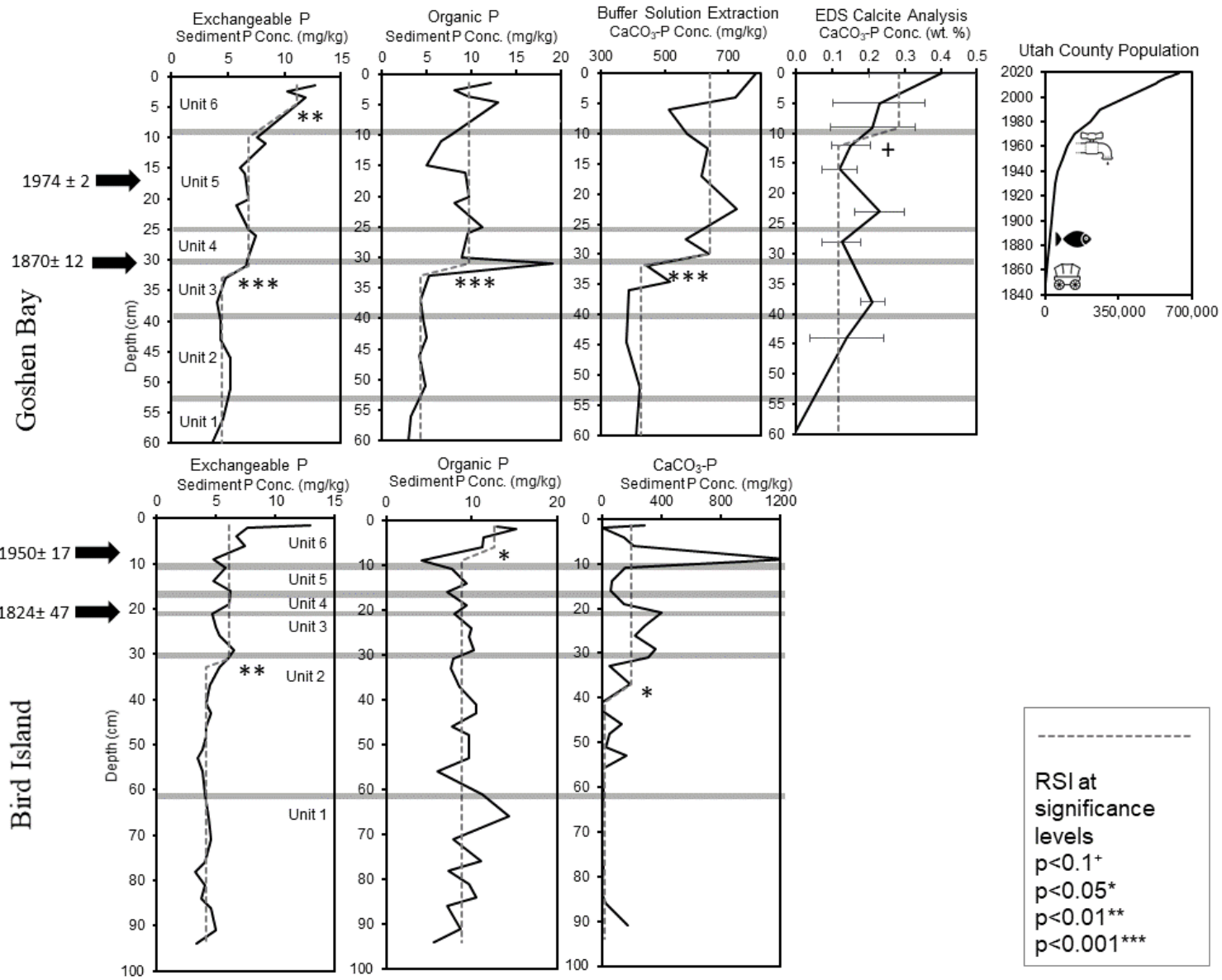
Figure 5. Sequential fractionation results for Goshen Bay and Bird Island cores, showing the exchangeable P (MgCl2-extractable), organic P (NaOH-extractable NRP), and carbonate P for Bird Island (0.5 HCl-extractable P), as well as the profile from targeted $CaCO_3$ analyses in Goshen Bay sediments. Dotted lines indicate results of Regime Shift Analysis, where asterisks denote significance levels. Ages given from isotope models (see Materials and Methods). "Zero" values here represent nondetects by the instrument, not true zero.

Figure showing sediment phosphorus concentration profiles for Provo Bay and North sites. Top row (Provo Bay): Exchangeable P, Fe/Mn Oxide P, Organic P, CaCO₃-P, Refractory P, and Utah County Population. Bottom row (North): Exchangeable P, Fe/Mn Oxide P, Organic P, CaCO₃-P, Refractory P. Legend box: RSI at significance levels p<0.1+, p<0.05*, p<0.01**, p<0.001***.

Figure 6. Sequential fractionation results for Goshen Bay and Bird Island cores, showing the exchangeable P (MgCl2-extractable), organic P (NaOH-extractable NRP), and carbonate P for Bird Island (0.5 HCl-extractable P), as well as the profile from targeted CaCO₃ analyses in Goshen Bay sediments. Dotted lines indicate results of Regime Shift Analysis, where asterisks denote significance levels. Ages given from isotope models (see Materials and Methods). "Zero" values here represent nondetects by the instrument, not true zero.

Energy-dispersive X-ray Spectroscopy Analysis

Average P concentrations of all $CaCO_3$ grains from each sediment interval in the Goshen Bay core are reported in figure 7. The profile shows a net increase in $CaCO_3$-P concentrations up-core, and a shift in sample means occurs between 7.5 and 10.5 cm (1982 and 1964) from 0.11% to 0.3% P, (RSI = -0.288, p=0.072)). Most grains analyzed were either nondetects or 0.1 or 0.2% P by weight after removing C and Si from the spectra. A few grains had P content as high as 0.8%, mainly in the surface sample. Figure 8 is an SEM image of drop cast Goshen Bay sediments highlighting the distinct size class differences between detrital grains and biogenic materials versus the uniform authigenic $CaCO_3$, as well as a typical map of elements we used to distinguish $CaCO_3$ grains from other materials in the drop cast sediment sample, including Mg, Al, and Ca.
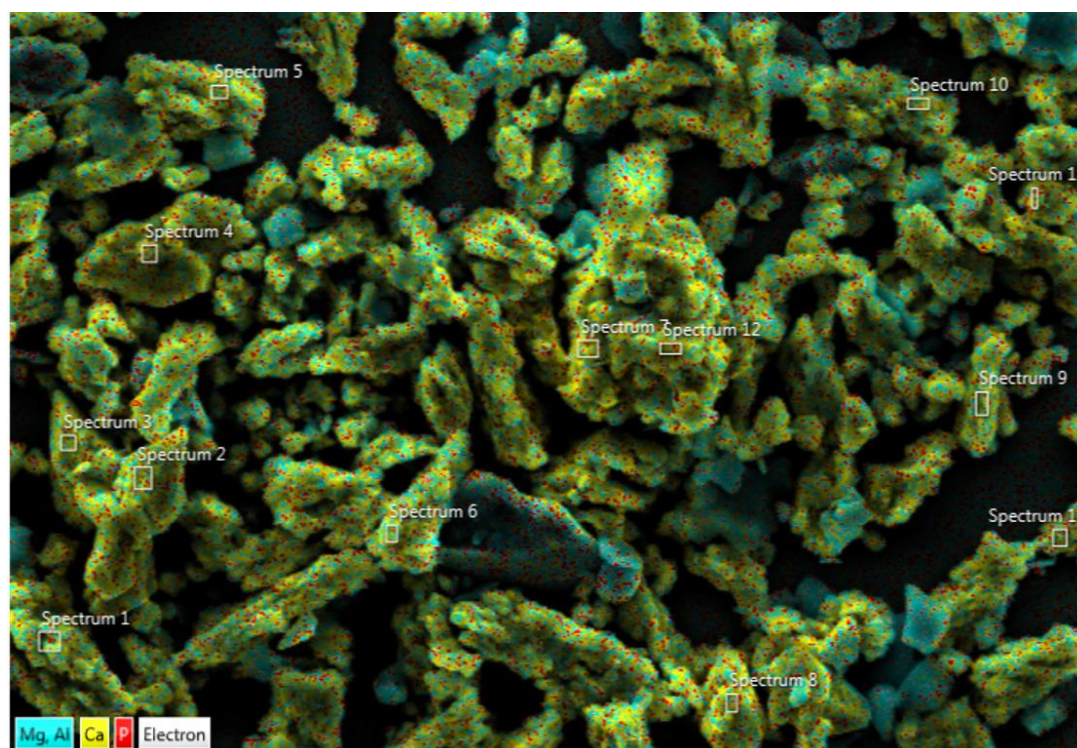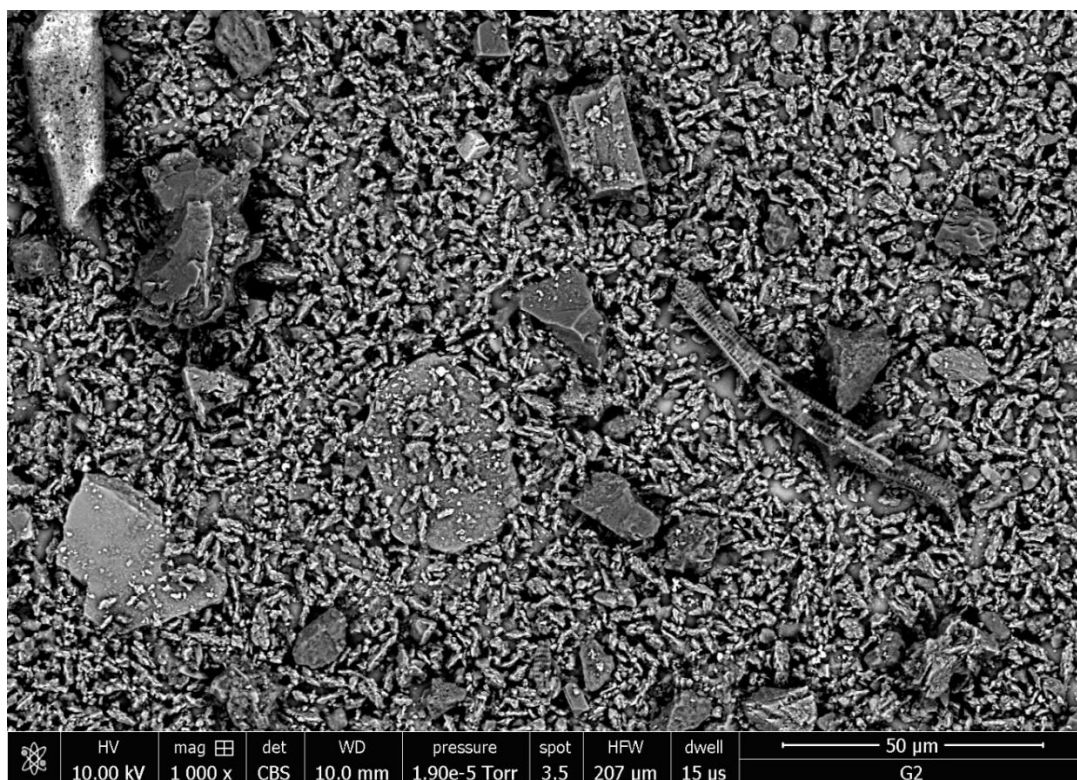
Figure 7. Backscatter SEM image demonstrating the two size classes of drop-cast Utah Lake sediments (top) and EDXA map overlay of another set of sediments showing Mg and Al in blue, Ca in yellow, and P in red. Squares labeled "Spectrum 1" and so on are the areas scanned for elemental composition.

Size-separated CaCO₃-Phosphorus Analysis

The buffer digestion dissolved between 51.7 and 178.1 mg of material from each of the samples. Concentrations of major cations extracted at this pH strongly suggest that this material is dominantly calcium carbonate. Whereas pure calcium carbonate is 40% calcium by weight, the total major cations measured here (Ca, Mg, Mn, Fe, Sr, Ba) ranged from 31.4% to 36.7%. The discrepancy between the total cations we measured and the idealized 40% cations for pure calcium carbonate are likely silica, residual water, other trace cations, or a result of Mg or Mn substitutions in the calcium carbonate, which would make the mass of cations in the carbonate slightly less than 40%. Calcium content in the dissolved material ranged from to 29.9% to 33.9%. The total concentration of the minor cations we measured increased slightly up core, from about 2.7% to about 3.5%.

The P concentration in the dissolved material approximately doubled throughout the interval of the core, ranging from 411 mg/kg at the deepest interval to 784 mg/kg at the shallowest interval (figure 5.) The trend of P:Ca ratios is similar, ranging from 0.0012 in the deepest sample to 0.0026 in the shallowest interval (figure X.) From the strong agreement between trends in P concentration in the dissolved material and overall P:Ca ratios, we can infer that the P extracted by the digestion is strongly associated with calcium carbonate.

DISCUSSION

The objectives of this study were to use several different approaches to reconstruct the P concentration history of Utah Lake, and then compare an established method for analyzing phosphorus in sediment cores with a novel proxy tool. The case of Utah Lake provided a prime opportunity for these comparisons because it is a waterbody which experiences harmful algal blooms due to excess P pollution. Because the lake is a valuable resource to a surrounding metropolitan population of over half a million residents, there is an impetus to compare historical and present nutrient conditions to inform ecological and water quality remediation efforts. The combined findings of these analyses suggest that phosphorus concentrations across the lake have increased in recent decades, corresponding in timing with changes to the lake from modern development. This signal of increasing P concentrations is strongest in regions with known recurrences of harmful algal blooms, including Provo Bay and Goshen Bay. There is less of a change in the northern region of the lake, which has likely experienced less eutrophication because it is a considerable distance from major population centers and associated WWTP and discharge sources. The differences across the lake may also reflect the effects of common carp introduction to the lake.

Evaluation of Methods

Sequential fractionation, which we applied to 87 sediment samples across all four of our cores, proved to be a valuable analysis process for interpreting P profiles in sediments. From this study, we know the relative differences between operational P fractions among differing regions of our study lake. In addition to spatial differences, we

were able to analyze the depth component of each of the target P fractions to offer insight into their changes over time.

There remains a number of fundamental limitations to the sequential fractionation of phosphorus and how the results of this study might be interpreted. Bacon and Davidson (2008) identified several potential issues that might arise during an operationally defined extraction scheme, writing about the extraction of trace and contaminant metals generally. In certain situations, sequential fractionation schemes can re-distribute the analyte among fractions, non-selectively extract the analyte, incompletely extract, or cause the precipitation of new compounds that might cause under-estimation in one step of the sequence and over-estimation in another. Previous research in the field has identified several of the above limitatations in the specific case of P. For example, Psenner and Jansson (1988) cautioned that citrate in the CDB reagent may solubilize some $CaCO_3$-P. Likewise, Hieltjes and Lilkjema (1980) recognized the potential for P extracted by NaOH to be carried over into calcium-bound P fractions if it induces co-precipitation of phosphorus with calcium carbonate. Whereas these authors recommend extracting $CaCO_3$-P prior to an NaOH extraction to avoid artifacts, Hupfer et al. (2009) suggest that unless a lake has been artificially treated by calcium or aluminum for remediation, this effect is likely minimal, and recommend extracting with NaOH prior to HCl. Altohugh it is beyond the scope of this study to evaluate the relative merits ofmultiple approaches to sequential extraction, the uncertainty surrounding the basic idea of the ordering of the sequence remains an issue. Indeed, the ordering of steps in a fractionation sequence might best depend on which fraction the researcher cares most to preserve from artifacts or other carry-over effects.

   The results of this study support the continued usage of sequential fractionation
for the study of marl lake nutrient history. The analysis allows for a characterization of
the types of compounds where P is stored within the sediment across differing lake
environments (e.g. varying proximity to pollution source), but of equal interest is the use
of this method to establish a vertical profile to understand both lake water quality history
and the fate and mobility of various P fractions. The separation of fractions which serve
as a record of past lake conditions (e.g. organic, refractory, and $CaCO_3$-P) from mobile
fractions (i.e. Fe/Mn oxide-P) remains effective. Still, one of the greatest challenges with
interpreting the results of sequential fractionation is determining how well each "target"
phase has been isolated. For example, an analysis of BD extractions for a suite of metals
revealed that although the extraction did appear to release some Fe and Mn (around 10
and 0.5 mg/L in the extract, respectively), there was around 100-200 mg/L of Ca in the
same solution. It is therefore difficult to definitively parse how much of the P in each
solution was associated with which elements.

   In an effort to explore the efficacy of a more streamlined approach to
reconstructing history, this study set out to explore novel approaches to working around
some of the inherent limitations of operationally-defined sequential fractionation.
SEM/EDS analysis of Utah Lake $CaCO_3$ grains is promising as an emerging method and
suggests an increase in P over time in Goshen Bay. The median P:Ca ratio among the
grains analyzed by EDS was higher than the median of ratios measured in the buffer
solution extraction of $CaCO_3$-P (0.006 and 0.001738 respectively). P:Ca ratios in
individual grains analyzed by EDS also had a more varied distribution (appendix 8). This
method, as current technology stands, is not adequately precise for detecting relative

elemental concentrations, and the results of our EDS analysis alone are not sufficiently robust to offer evidence for an up-core trend in Goshen. Still, the advantage for its potential uses in sediment core analysis lies in the precision of the microscopy for analyzing only the mineral type of interest. Whereas sequential fractionation methods only allow for the operational separation of various P species, it was relatively simple with EDS maps overlaying the SEM imagery to identify non- $CaCO_3$ mineral species (e.g. iron oxides, aluminum oxides, apatite), and avoid them. In the example of Goshen Bay sediments, this distinction is of particular interest because although calcium carbonate is more abundant than most other minerals in our drop cast sample mounts, the most concentrated groupings of P on the EDS maps were typically associated with non-carbonate minerals.

The buffer solution extraction of the <10 µm Goshen Bay sediments is the most reliable of our $CaCO_3$-P profiles because it had the least opportunity for carry-over and artifacts from other P fractions. The separation of size fractions was effective in concentrating the mineral of interest. In addition, the measurements taken in this analysis allowed us to measure the mass of material dissolved in the extract, which offered a more precise calculation of $CaCO_3$-P concentrations than in our sequential fractionation scheme. Further, the pH of this mildly acidic acetic acid solution was sufficient to dissolve $CaCO_3$-P but was overall less aggressive than an HCl extraction. We are confident, therefore, that the data resulting from this analysis indicate an increase in P concentration in Utah Lake $CaCO_3$-P, concurrent in timing with known potential drivers of phosphorus pollution in this study lake.

An important consideration for analyzing the $CaCO_3$ fraction in sediment cores is the possibility of secondary calcium mineral formation in the post-depositional environment. The formation of secondary minerals in young (<500 years) sediment may warrant further investigation, especially because the mobilization of the Fe/Mn oxide-bound P fraction could release P into the pore water which could mineralize as $CaCO_3$-P co-precipitates or other minerals. However, basic examination of sediment texture by drop cast showed no signs of early cementation between individual $CaCO_3$-P grains. Even if some mobilized P were to co-precipitate with secondary CaCO3, it would not cause an up-core increase in the CaCO3-P fraction because the release of P from deep, anoxic sediments is a constant effect, meaning that sediments at any given interval will have an opportunity to be exposed to mobilized P in the pore water as accumulation proceeds. We therefore consider any increase up-core in the CaCO3-P fraction to reflect primary authigenic mineralization.

Implications for Utah Lake

The most prominent increases in phosphorus across each of the four cores occur around the beginning of units 4 and 5 (figures 3-5). Many of the sequential fractionation profiles, as well as the size-separated buffer solution extraction, show an increase in mean P concentrations at this point according to the regime shift indicator (RSI) calculation. The Goshen Bay dating model places the start of these units about the 1860s, when wastewater would have first been introduced to the lake, and when common carp began to cause major shifts in parts of the lake with historically robust macrophyte communities (King 2019).

Among the four cores, Provo Bay appears to be the most phosphorus rich with respect to exchangeable P, organic P, and $CaCO_3$-P . However, $CaCO_3$-P in Provo Bay appears to be far higher than North or Goshen Bay. Comparing Provo Bay and North HCl-extractable P with the $CaCO_3$ analysis of the Goshen Bay core, Goshen Bay and Provo Bay experience greater P concentrations than the north part of the lake, which is expected due to its distance from wastewater effluent and agricultural runoff, as well as contemporary Utah Lake water quality data (Utah Department of Environmental Quality, 2021). Of all the cores, Provo Bay appears to have the highest concentrations of $CaCO_3$-P at its peak, even after considering that the best $CaCO_3$-P data set for Goshen Bay uses a slightly different metric from the other three cores (appendix 9).

Trends across all the profiles most strongly point to changes in the phosphorus profile beginning around 30 to 35 cm depth, or the mid- to late-19th century, based on our age-depth models. In the North and Goshen Bay cores, organic-P increases from this depth, indicating an increase in biological production, even outside of Provo Bay. In the Provo Bay core, this increase is manifest a little later in the timeline, around 22 cm depth, or the early 20th century. $CaCO_3$-P increases in Provo Bay by about 300%, and in Goshen Bay by slightly less than 100%. There is only a slight increase in this fraction in the North core. This analysis presents evidence that cultural eutrophication has occurred in Utah Lake, concentrated in areas of recurring HABs. These differences correspond with existing Utah Lake water quality data that show considerably higher surface water P concentrations in Provo Bay, and to some extent Goshen Bay, than elsewhere in the lake (Utah Department of Environmental Quality, 2021).

The Provo Bay core is an insightful record of the region of the lake which currently has the highest phosphorus concentrations. The accompanying age-depth model indicates that the important contact between units 3 and 4 (appendix 5) likely could represent a change which happened in the decades following the arrival of settlers. It would have taken a sudden and dramatic shift in the depositional environment of Provo Bay to cause such a sudden and stark change, and likely some sort of anthropogenic disturbance, although natural variability is possible. For example, Brimhall & Merritt (1981) attributed a shift from sandy peat texture to carbonate mud ~5,000 years B.P. to the dry climate of the altithermal, or the Holocene climatic optimum. The more probable cause for this shift was identified as the introduction of common carp in King (2019), although lake elevation manipulation, which began less than a decade prior to carp introduction, may have compounded this effect. In any case, the bay appears to have been historically macrophyte dominated.

Natural variability in water column ion concentration as well as sediment Ca concentration are important to consider alongside any trends or variation in P concentration. The range of total dissolved solids, for example, spans approximately 700-1,300 mg/L (Utah Division of Water Quality, 2021). Brimhall and Merritt (1981) demonstrated how well fluctuations in lake surface elevation correspond with percent sediment calcium in one core collected 2.5 miles west of the historic Geneva steel mill in Vineyard, Utah. Calcium concentrations fluctuated between about 18-32% in the top 450 cm of the core. Such variability could lead to enormous changes in $CaCO_3$-P concentrations in a traditional sequential fractionation scheme where sediment P concentrations are only calculated with respect to initial mass of sample. Natural

variability underscores the importance of accounting for mass of material extracted as well as Ca:P ratios for analyzing this fraction as a record of past water column chemistry.

Organic P also increases in the post-1849 era across all our cores, suggesting increased accumulation of P as algal cells or other biological materials. The same is also true of the exchangeable P fraction, which may indicate increased deposition as well as recycling of P in the sediments. Still, the vast majority of total P in each of these cores is in the form of Fe and Mn-oxide P, $CaCO_3$-P, and refractory P. In the Provo Bay and North cores (figure 4), there is a clear trend of increasing Fe/Mn-oxide P, meaning that this fraction is probably serving as a significant source of legacy P. In contrast, the $CaCO_3$ and refractory fractions represent long-term P storage, with $CaCO_3$ storing an increasing amount of P over the time intervals represented in these cores.

Recent calculations of the P mass balance in Utah Lake estimate 183 tons per year are loaded into the lake, and 13.5 tons are loaded out, meaning that the retention rate

$$\frac{1 - P \; loaded \; out}{P \; loaded \; in}$$

is approximately 0.93, a number which can fluctuate with relative changes in P speciation or algal activity. If we assume that much of the P permanently retained in the lake is sequestered in the form of $CaCO_3$-P co-precipitates, then changes in $CaCO_3$ concentrations offer some idea as to how loading might have changed over time. For example, the youngest sediments in the Goshen Bay core would suggest that 238,000 kg/year P is stored in the lake as calcium carbonate, compared to 116,000 pre-disturbance. The former value is clearly higher than the P loading calculated in budgets, but Goshen Bay is also relatively concentrated in P and HABs, so it would be expected to

represent a more extreme example. The same comparison in pre-disturbance versus recent sediments in the North core, which has not been as frequent a site of HABs, suggest a change from 79,000 kg/year buried as $CaCO_3$ to 92,000 kg/year in recent sediments.

P burial estimates taken from just a few points around the like are clearly restricted in how they can be extrapolated across the whole lake, but they serve to illustrate a possible range for how much P loading might have changed in the last 170 years. For example, if the retention rate (0.93) is applied to P burial estimates in North core, the P loading might have changed from 85,000 kg/year into the lake to 99,000 kg/year. This value is likely conservative based on the total lake P budget. The same retention rate applied to the Goshen Bay core suggests a greater change in loading from 125,000 kg/year P loading into the lake to 256,000 kg/year in recent years.

Randall et al. (2019) generated an interpolated map of Utah Lake surface sediment TP concentrations which shows that although Goshen Bay sediment concentrations are moderately elevated in P concentration, they are not exceptional either. Therefore, the data presented in this study offer evidence that P loading into Utah Lake has increased by several tens of thousands of kg per year, if not in the realm of a hundred thousand. P loading reductions from point- and non-point sources on this order of magnitude will be required in tandem with several other restoration efforts to control HABs more effectively in the future.

CONCLUSION

Records of $CaCO_3$-P in sediment cores collected from Utah Lake indicate that phosphorus concentrations increased to varying degrees, corresponding with modern population growth in the watershed began in the mid-to-late 19th century. This study suggests that in the regions of Utah Lake most affected by harmful algal blooms, phosphorus concentrations might have increased by nearly 100% in Goshen Bay, and likely more in Provo Bay, in the last two-hundred years. There are several anthropogenic disturbances which have contributed to ecological changes in Utah Lake, but the lake phosphorus concentrations demonstrated here are likely a primary driver of these changes. Reducing P concentrations in the lake will likely be required as part of broader conservation and restoration efforts in Utah Lake. Because Utah Lake is not unique among marl lakes which experience cultural eutrophication, the novel methods used here represent a promising new approach to be built upon for reconstructing historical lake P concentrations in similar lacustrine systems.

REFERENCES

Bacon, J. R., & Davidson, C. M. (2008). Is there a future for sequential chemical extraction? Analyst. **133**: 25–46. https://doi.org/10.1039/b711896a

Blaauw, M., & Christen, J. A. (2011). Flexible paleoclimate age-depth models using an autoregressive gamma process. Bayesian analysis. **6**: 457-474.

Bradshaw, E. G., & John Anderson, N. (2001). Validation of a diatom-phosphorus calibration set for Sweden. Freshwater Biology. **46**: 1035–1048. https://doi.org/10.1046/j.1365-2427.2001.00732.x

Carignan, R., & Flett, R. J. (1981). Postdepositional mobility of phosphorus in lake sediments 1. Limnology and Oceanography. **26**; 361-366.

Dean, W. E. (1981). Carbonate Minerals and Organic Matter in Sediments of Modern North Temperate Hard-Water Lakes. Society of Economic Paleontologists and Mineralogists. 213–231.

Devey, M., Brahney, J. (2019) Calcium carbonate co-precipitation with phosphorus: developing a novel technique for reconstructing historic lake trophic states [Conference Presentation]. Spring Runoff Conference, Logan, UT, United States.

Einsele, W. (1936). Über die Beziehungen des Eisenkreislaufs zum Phosphatkreislauf im eutrophen See. Archiv für Hydrobiologie. **29**: 664-686.

Einsele, W. (1938). Uber Chemischen and kolloidchemische vorgange in Eisen. Phosphatsystemn unter Limnochemischen and Limnogeologischen Gesicht Spunkten.

Gilbert, G. K. (1890). Lake Bonneville. **1**. United States Geological Survey.

Ginn, B. K., Rühland, K. M., Young, J. D., Hawryshyn, J., Quinlan, R., Dillon, P. J., & Smol, J. P. (2012). The perils of using sedimentary phosphorus concentrations for inferring long-term changes in lake nutrient levels: Comments on Hiriart-Baer et al., 2011. Journal of Great Lakes Research. **4**: 825-829.

Hamilton, S. K., Bruesewitz, D. A., Horst, G. P., Weed, D. B., & Sarnelle, O. (2009). Biogenic calcite-phosphorus precipitation as a negative feedback to lake eutrophication. Canadian Journal of Fisheries and Aquatic Sciences. **66**: 343–350. https://doi.org/10.1139/F09-003.

Hieltjes, A. H., & Lijklema, L. (1980). Fractionation of inorganic phosphates in calcareous sediments. American Society of Agronomy, Crop Science Society of America, and Soil Science Society of America. **9**: 405-407.

Horns, D. (2005). *Utah Lake Comprehensive Management Plan Resource Document*. 1–109.

Hupfer, M., Gächter, R., & Giovanoli, R. (1995). Hupfer, M., Gächter, R., & Giovanoli, R. (1995). Transformation of phosphorus species in settling seston and during early sediment diagenesis. Aquatic Sciences, **57**: 305–324.

Hupfer, M., Zak, D., Roβberg, R., Herzog, C., & Pöthig, R. (2009). Evaluation of a well-established sequential phosphorus fractionation technique for use in calcite-rich lake sediments: identification and prevention of artifacts due to apatite formation. Limnology and Oceanography: Methods. **7**: 399-410.

Ingall, E. D., Schroeder, P. A., & Berner, R. A. (1990). The nature of organic phosphorus in marine sediments: New insights from 31P NMR. Geochimica et Cosmochimica Acta. *54*: 2617-2620.

Ishikawa, M., & Ichikuni, M. (1981). Coprecipitation of phosphate with calcite. Geochemical Journal. **15**: 283-288.

Judd, H. L. (1997). Utah's lakes and reservoirs: inventory and classification of Utah's priority lakes and reservoirs. Utah Department of Environmental Quality, Division of Water Quality.

Juggins, S., Anderson, N. J., Hobbs, J. M. R., & Heathcote, A. J. (2013). Reconstructing epilimnetic total phosphorus using diatoms: statistical and ecological constraints. Journal of Paleolimnology. **49**: 373-390.

King, L. R. (2019). The Response of Utah Lake's Plant and Algal Community Structure to Cultural Eutrophication.

Kitano, Y., Okumura, M., & Idogaki, M. (1978). Uptake of phosphate ions by calcium carbonate. Geochemical Journal. **12**: 29-37.

Kleiner, J. (1988). Coprecipitation of phosphate with calcite in lake water: A laboratory experiment modelling phosphorus removal with calcite in Lake Constance. Water Research. **22**: 1259–1265. https://doi.org/10.1016/0043-1354(88)90113-3

Mortimer, C. H. (1941). The exchange of dissolved substances between mud and water in lakes. Journal of ecology. **29**: 280-329.

Murphy, T. P., Hall, K. J., & Yesaki, I. (1983). Coprecipitation of phosphate with calcite in a naturally eutrophic lake. Limnology and Oceanography. **28**: 58–69. https://doi.org/10.4319/lo.1983.28.1.0058

Ostrofsky, M. L. (2012). Differential post-depositional mobility of phosphorus species in lake sediments. Journal of paleolimnology. **48**: 559-569.

Otsuki, A., & Wetzel, R. G. (1972). Coprecipitation of Phosphate with Carbonates in a Marl Lake. Limnology and Oceanography. **17**: 763–767.

Oviatt, C. G. (1997). Lake Bonneville fluctuations and global climate change. Geology. *25*: 155-158.

Pełechaty, M., Pukacz, A., Apolinarska, K., Pełechata, A., & Siepak, M. (2013). The significance of Chara vegetation in the precipitation of lacustrine calcium carbonate. Sedimentology. **60**: 1017–1035. https://doi.org/10.1111/sed.12020

Persson, G., & Jansson, M. (1988). Phosphorus in freshwater ecosystems.

Randall, M. C. (2017). Characterizing the Fate and Mobility of Phosphorus in Utah Lake Sediments.

Randall, M. C., Carling, G. T., Dastrup, D. B., Miller, T., Nelson, S. T., Rey, K. A., … Aanderud, Z. T. (2019). Sediment potentially controls in-lake phosphorus cycling and harmful cyanobacteria in shallow, eutrophic Utah Lake. PLOS ONE. 14. e0212238. https://doi.org/10.1371/journal.pone.0212238

Schindler, D. W. (2012). The dilemma of controlling cultural eutrophication of lakes. Proceedings of the Royal Society B: Biological Sciences. **279**: 4322-4333.

Schindler, D. W., Carpenter, S. R., Chapra, S. C., Hecky, R. E., & Orihel, D. M. (2016). Reducing phosphorus to curb lake eutrophication is a success. Environmental Science & Technology. **50**: 8923-8929.

Thiel, V., Merz-Preiß, M., Reitner, J., & Michaelis, W. (1997). Biomarker studies on microbial carbonates: Extractable lipids of a calcifying cyanobacterial mat (Everglades, USA). Facies. **20**: 163–172. https://doi.org/10.1007/bf02536882

Thompson, J. B., Schultze-Lam, S., Beveridge, T. J., & Des Marais, D. J. (1997). Whiting events: Biogenic origin due to the photosynthetic activity of cyanobacterial picoplankton. Limnology and Oceanography. **42**: 133–141. https://doi.org/10.4319/lo.1997.42.1.0133

Ure, A. M. (1991). Trace element speciation in soils, soil extracts and solutions. Microchimica Acta. **104**: 49-57.

U.S. Census Bureau quickfacts: Utah County, Utah. Retrieved November 15, 2021, from https://www.census.gov/quickfacts/fact/table/utahcountyutah/PST045219.

Utah Department of Environmental Quality, Utah Lake TMDL60–61 (2007). Salt Lake City, UT; PSOMAS.

Utah Department of Environmental Quality, Utah Lake Data. Retrieved 21 Nov 2021, from https://github.com/KateriSalk/UtahLakeData

Vollenweider, R. A. (1970). Scientific fundamentals of the eutrophication of lakes and flowing waters, with particular reference to nitrogen and phosphorus as factors in eutrophication. OECD REPORT, SEPTEMBER 1970. 159.

APPENDICES

Appendix 1. Raw ^{137}Cs activity in at each sediment depth for the Provo Bay core (left) and Goshen Bay (right).
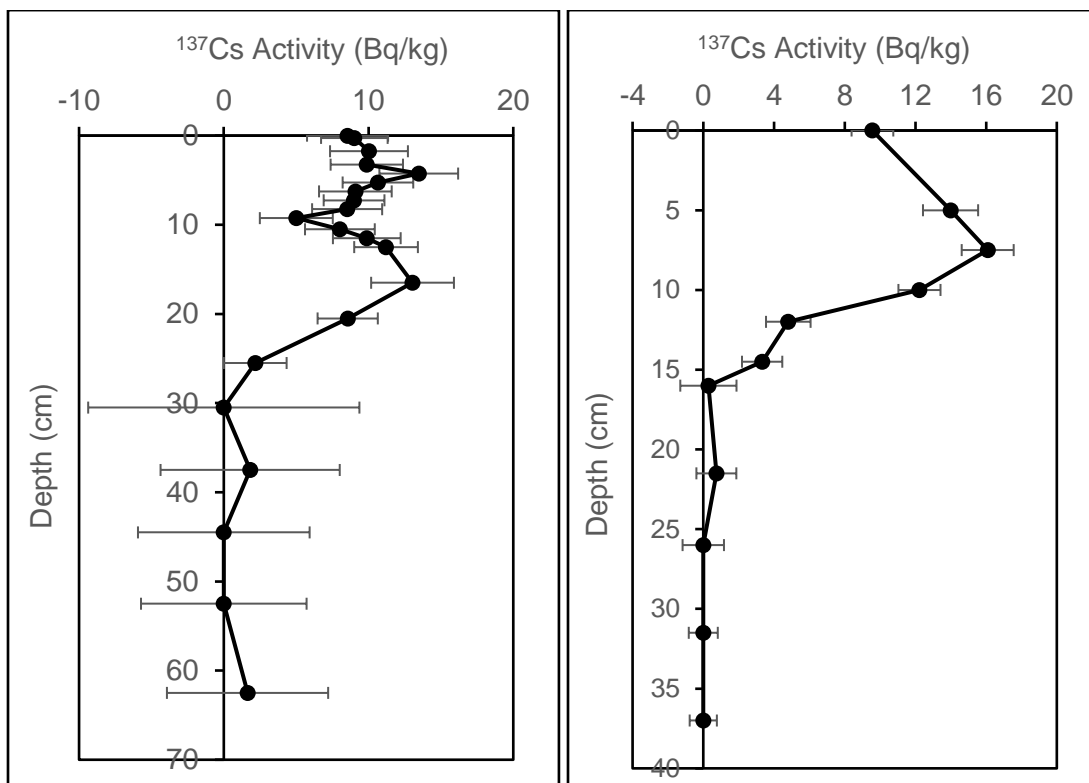
Appendix 2. LOI 1000 °C profiles for each core.
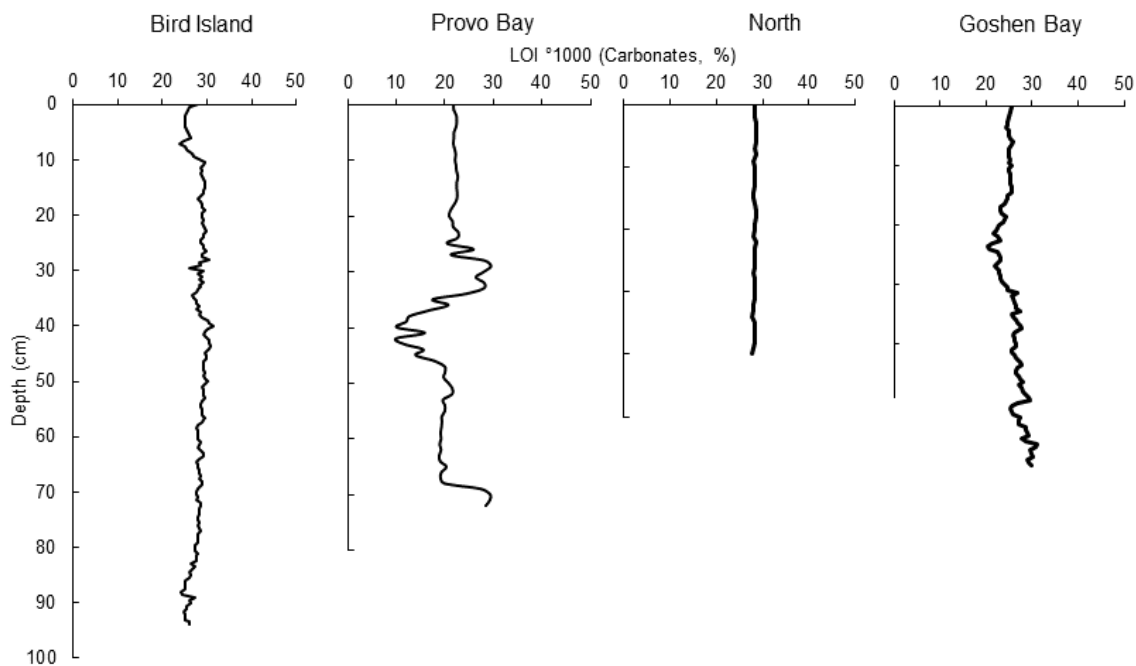
Appendix 3. Inorganic sediment profiles for each core.
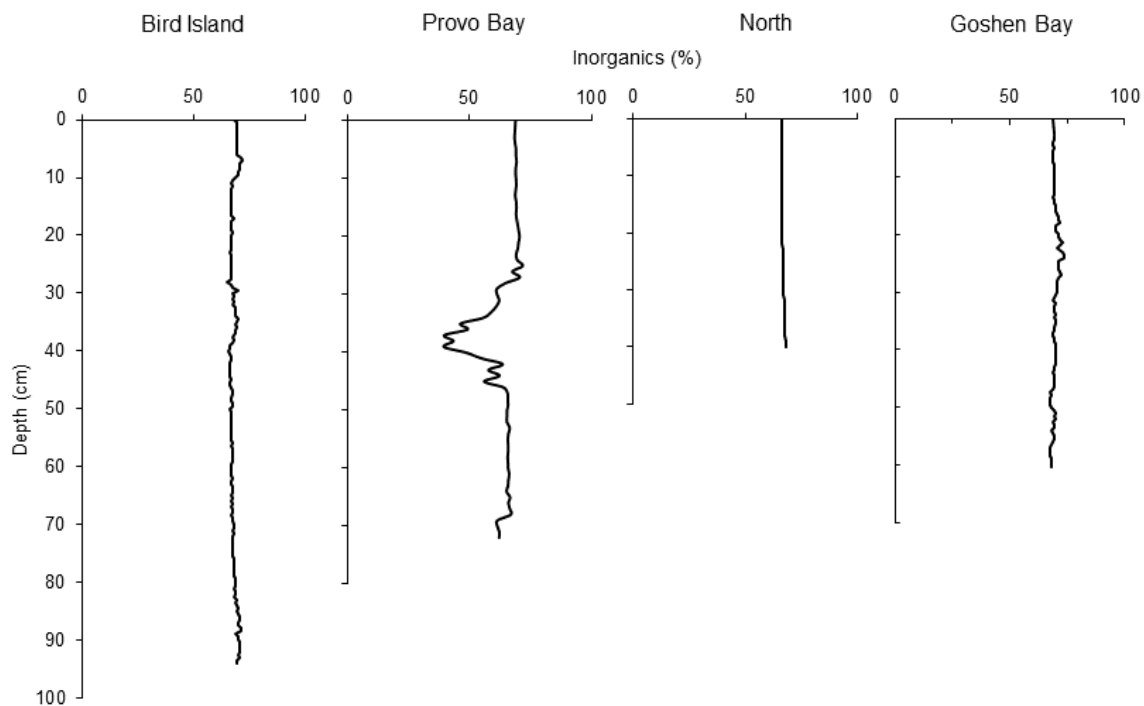
Appendix 4. Sediment moisture content profiles for each core.
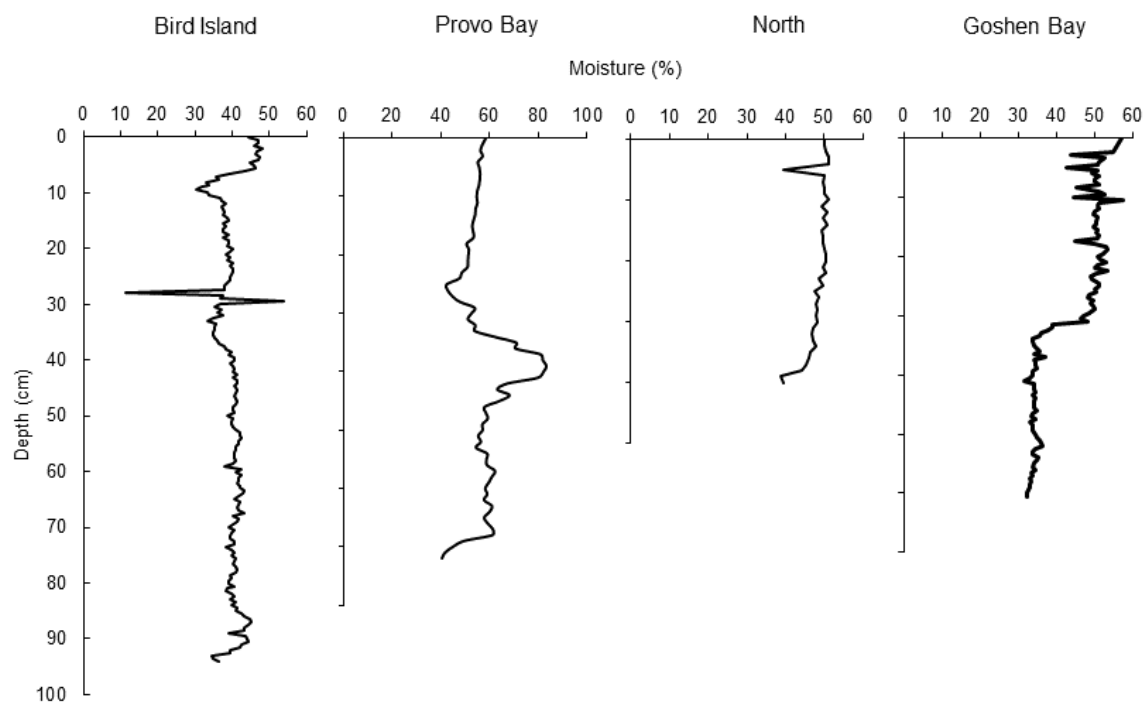
Appendix 5. Stratigraphic column of the Provo Bay core with units based on physical description of the split core.

| Images	Units	m	Intervals	Symbols	Description
	5	0.1 / 0.2 / 0.3		(void)	**0.0 m-0.012 m** Foam Spacer **0.012 m-0.311 m** Silt, calcareous
	4				**0.311 m-0.362 m** Silt, calcareous, with abundant gastropod shells
	3	0.4			**0.362 m-0.446 m** Predominantly vegetative material; sediment characteristics difficult to distinguish
	2	0.5 / 0.6			**0.446 m-0.695 m** Silt, calcareous, with organic matter
	1	0.7 / 0.8 / 0.9			**0.695 m-0.745 m** Gradational contact into silt, calcareous

Appendix 6. Efficiency and consistency of extractions on five different sub-samples of SRM-2702 Inorganics in Marine Sediments. The top bar indicates the certified value of total P in the sediment material. The remaining five bars indicate the values for each of five P fractions in the SRM.
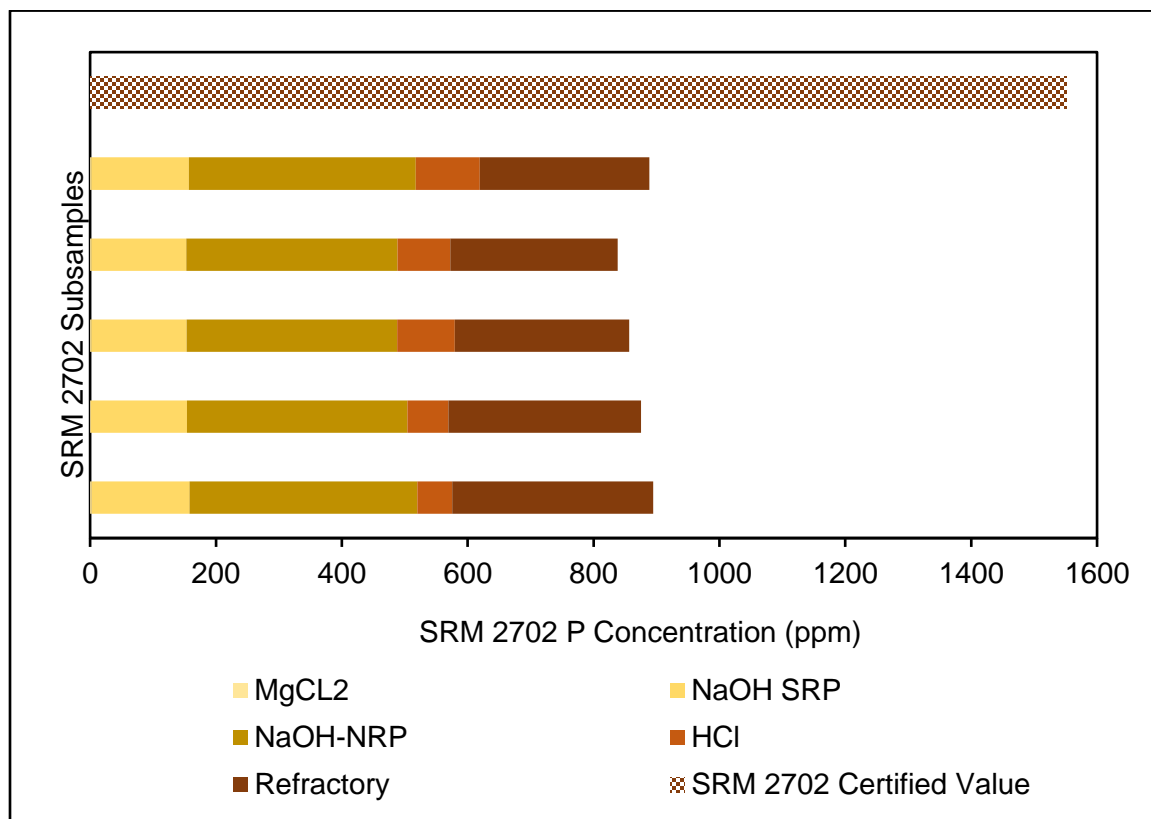

Appendix 7. Table describing the efficiency and consistency of extractions on five sub-samples of SRM 2702 - Inorganics in Marine Sediments. Note that the BD extraction on this material had a lower P concentration than the reagent blank. Values given in ppm P. The certified P concentration of this material is 0.1552%.

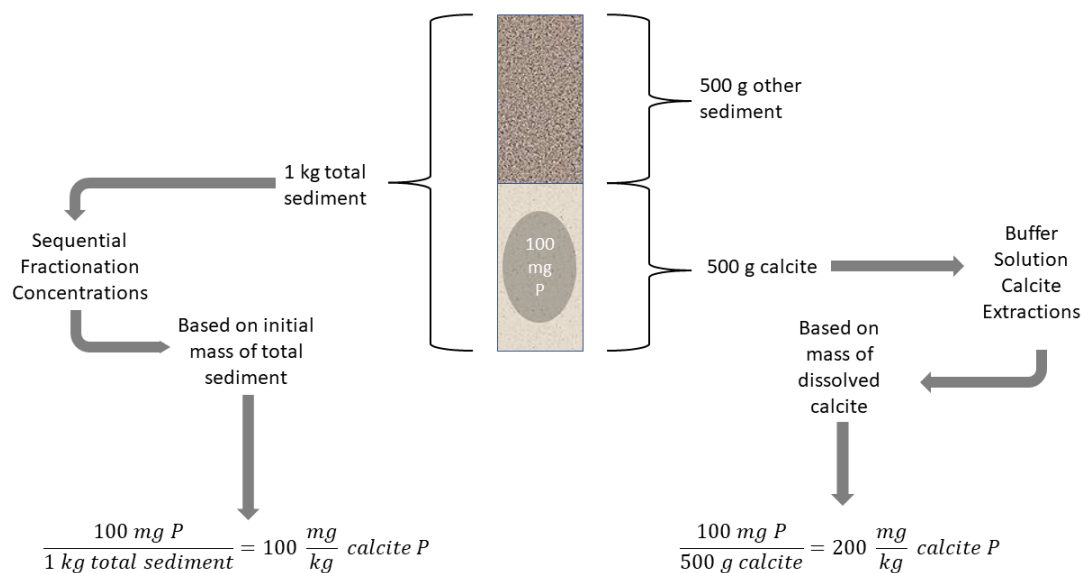| Subsample	MgCl2	BD	NaOH-SRP	NaOH-NRP	HCl	Refractory	Total	Total (excluding BD)
A	2.20	-7.04	155.64	362.20	55.60	319.32	887.92	894.96
B	1.55	-19.85	152.12	350.34	65.39	305.82	855.36	875.21
C	1.74	-54.90	151.79	334.64	91.22	277.37	801.86	856.76
D	1.63	-27.04	151.18	335.52	83.81	265.90	810.99	838.03
E	1.71	15.25	154.99	360.62	101.69	269.37	903.64	888.38
Mean	1.77	-18.72	153.14	348.66	79.54	287.55	851.95	870.67
SD	0.254	25.84	2.0207	13.21	18.83	23.70	45.176	23.361
RSD	0.144	-1.38	0.013	0.038	0.237	0.0824	0.0530	0.0268

Appendix 8. Efficiency of extractions of five sub-samples of the same sediment core intervals. The total P was determined by dry oxidation and extraction by HCl and analysis by ICP-MS. The second bar is the total of all P extracted into each of the five fractions.
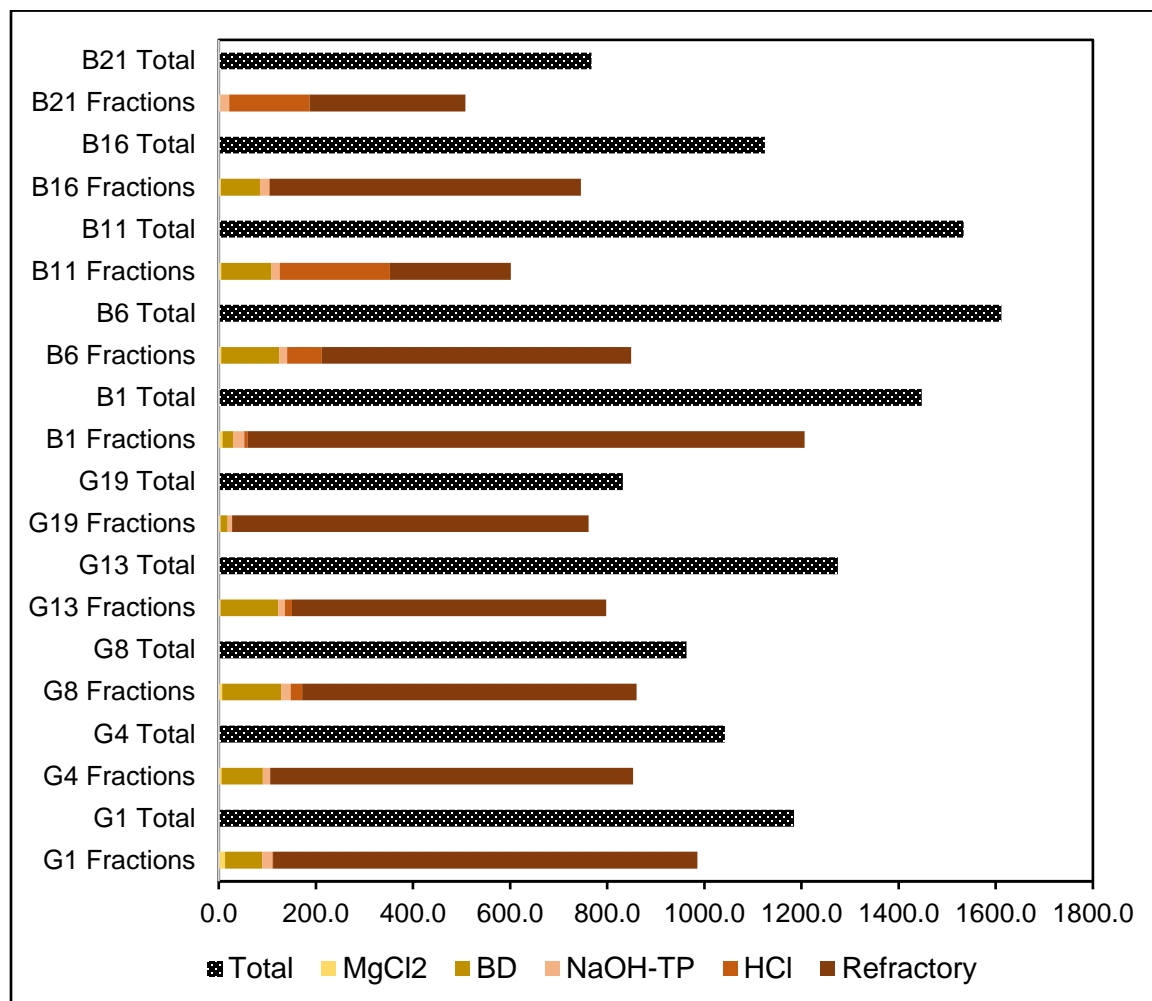
Appendix 9. Distribution of P:Ca ratios in individual calcite grains measured by EDS (nondetects excluded). Many of the highest ratios come from the first analysis of the shallowest sample (Goshen Bay 0-2.5 cm), which was duplicated and yielded slightly lower P concentrations and P:Ca ratios.
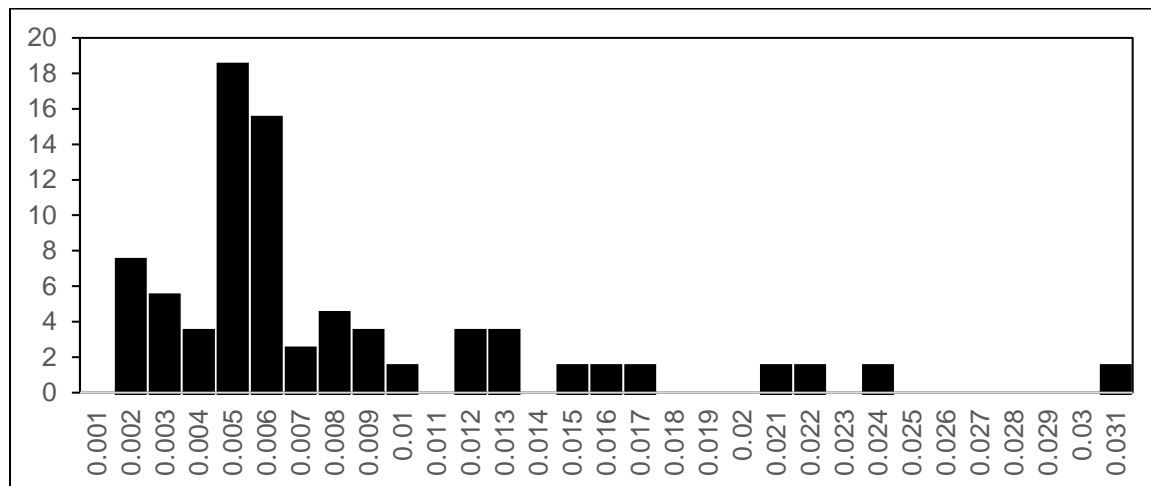
Appendix 10. Diagram showing the difference between the metrics used for our sequential fractionation data versus the buffer solution extraction of calcite-P.

$$\frac{100 \ mg \ P}{1 \ kg \ total \ sediment} = 100 \ \frac{mg}{kg} \ calcite \ P$$

$$\frac{100 \ mg \ P}{500 \ g \ calcite} = 200 \ \frac{mg}{kg} \ calcite \ P$$

ProQuest Number: 29067526

INFORMATION TO ALL USERS
The quality and completeness of this reproduction is dependent on the quality
and completeness of the copy made available to ProQuest.